Propellants,
Explosives,
Pyrotechnics

Full Paper

Detonation Wave Propagation in Double-layer Cylindrical High Explosive Charges

Xian-feng Zhang,* Zheng-xiang Huang, Liang Qiao

School of Mechanical Engineering, Nanjing University of Science and Technology, Nanjing 210094 (P. R. China)
e-mail: lynx@mail.njust.edu.cn

Received: January 7, 2010; revised version: May 28, 2010

DOI: 10.1002/prep.201000004

Abstract

The flow fields associated with regular and irregular reflections of detonation waves in double-layer cylindrical (DLC) high explosives (HE) are analyzed, and an analytical model for predicting the detonation wave configurations is proposed. Regular reflection and three-shock Mach reflection during detonation wave propagation are discussed. Calculated results of pressure, flow velocity, and specific volume are presented and the Mach stem height is also determined based on mass conservation. The corresponding numerical simulation based on the Lee–Tarver model is developed to generate data comparable with an ordinary cylindrical charge. It is shown that steady convergent detonation wave propagation occurs in the DLC charge. The maximum pressure up to 4.0 times of Chapman–Jouguet (CJ) pressure is reached at the collision point related to the Mach reflection, and the predictions based on the proposed model correlate well with corresponding numerical results.

Keywords: Detonation Wave, Double-layer Charge, Explosion Mechanism, Mach Reflection, Overdriven Detonation

1 Introduction

Due to requirements of the material processing, explosion synthesis of new materials, generation of high velocity projectiles, and various ways using high explosives (HE) to obtain an ultra-high pressure have been studied by many researchers in recent years. However, the energy of an HE charge depends on its own property, and hence its energy is limited. Hence, many researches focus on improving the capacity usage ratio of HE charge. Consulting the related literature, it is considered that the maximum detonation wave due to overdriven detonation might be twice as fast as the normal detonation velocity. This overdriven detonation process can be realized by using high-speed flying plate impact, initiated on the outer surface of a cylindrical or spherical HE charge and Mach reflections of detonation wave. A double-layer cylindrical (DLC) charge is an efficient way to achieve stable convergent detonation wave propagation with overdriven detonation. The illustration of DLC charge is shown in Figure 1. The inner cylindrical HE charge is surrounded by a concentric HE cylinder with high detonation velocity (D_O). The charge was initiated at annular surface at one end of the outer-layer charge. Because of higher detonation velocity of the outer-layer charge, a conical detonation wave converges on the axis of the cylinder as the detonation progresses, and generates regular reflection or Mach reflection at the symmetry axis of the charge.

DLC charge is a simple way to obtain a convergent detonation wave, and it is of high value in shaped charge, high-speed flying plate acceleration and explosion synthesis of new materials development. Research groups all over the world have carried out extensive research work on detonation wave propagation of DLC charges. As early as 1978, Müller [1] conducted the Mach reflection test of detonation waves in DLC charges by flash X-ray radiography. A strong detonation of Mach disk was observed in the inner layer of an HE specimen. Held [2] and Adadurov [3] presented the detonation wave shape of DLC charge using high-speed rotating-mirror streak camera with inner charge of TNT (Trinitrotoluene), glass and HMX/Binder(85/15), etc. Liu et al. [4–7] derived the equation of state of detonation products at an overdriven detonation state. Numerical studies of overdriven detonations by Mach reflections of detonation waves were also carried out. Otsuka et al. [8], Itoh [9], and Hamada et al. [10] used a manganin gauge and optical fibers to measure the detonation velocity and pressure at overdriven detonation of double cylindrical HE charges. A pressure four times higher than the normal detonation pressure (the Chapman–Jouguet (CJ) pressure) was obtained in their studies. Kato et al. [11] carried out numerical and experi-

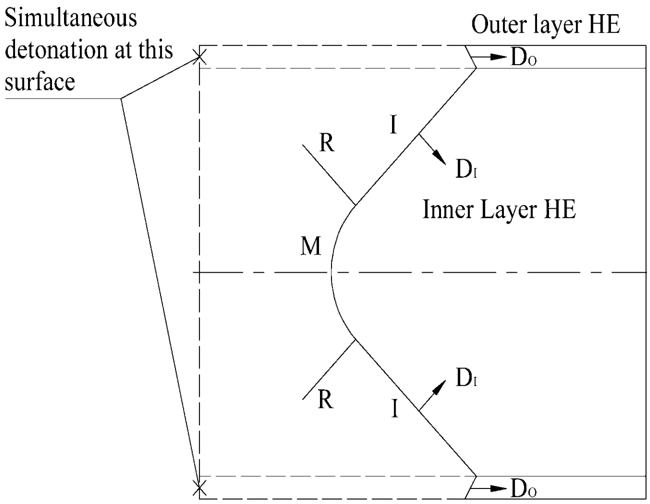

Figure 1. Configuration of DLC HE.

mental studies on DLC shaped charges by using tungsten loaded high-density PBX as an inner charge. The experimental results showed that the initial jet velocity and jet penetration velocity were significantly increased by using DLC shaped charges. Zhang et al. [12] presented a numerical simulation of jet formation and penetration of DLC shaped charge, the results showed that jet tip velocity and kinetic energy were increased by about 20 %. Consulting the related literature, limited analytical results of the detonation behavior were available for DLC charge. Analytical models and insight simulation were rarely used to describe the detonation wave propagation in DLC charges.

In this paper, a theoretical analysis of detonation wave propagation in DLC charges was presented. The velocity and angle of the conical detonation wave in DLC charges were calculated as a function of parameters of the outer and inner layer charges. The flow fields associated with regular and irregular reflection of detonation were analyzed, and an analytical model for determining Mach stem height was proposed. Numerical simulations based on ignition and growth model were conducted by using AUTODYN® software, which were compared with theoretical analysis results.

2 Analysis of Detonation Wave Propagation in DLC Charges

2.1 Propagation Description of Detonation Waves in DLC Charges

As shown schematically in Figure 1, the outer layer charge is initiated with a velocity of D_O which is higher than that of the inner charge. A conical detonation wave propagates in the inner layer charge as the detonation is progressing. Due to the shock induced by initiation of outer layer HE charge, the detonation wave in the inner charge delays to that of outer layer charge, and conical detonation wave propagates with a larger incident angle at beginning of detonation. With the detonation progressing, the detonation wave will satisfy a steady state condition and propagates with a constant shape ultimately. Because of the velocity difference of the two charges, there are two cases in propagation of detonation wave in DLC charge. In the first case, the incident angle ψ_I, which is defined by D_O and D_I, is less than the critical angle ψ_{IC} for Mach reflection. There will be a regular reflection of detonation wave in inner charge at axial line, propagating with a constant shape ultimately. The second case is that $\psi_I > \psi_{IC}$, regular reflection is not possible and Mach reflection will be expected to occur in this case.

From the descriptions above, the ultimate state of detonation wave in DLC charge is decided by parameters of two layers charge. Most of HE used by military have a CJ detonation velocity of 6500–10000 m s^{-1}, and the velocity ratio of two layer charges is always smaller than 1.5. The detonation wave always propagates with $\psi_I > \psi_{IC}$ and Mach reflection is expected to occur in the inner charge. The mathematical description of propagation and Mach reflection of detonation wave in DLC charge will be presented in the subsequent sections.

2.2 Mathematical Description of Detonation Waves in DLC Charges

The detonation wave configuration of DLC charge is shown schematically in Figure 2, in which the incident detonation front (I) intersects with the reflected shock (R) at O, a point on the line of collision. From the detonation reflection description in condensed HE of Dunne [13,14] and Sternberg and Piacesi [15], the parameters of each region are described as follows. The parameters between the detonation-front reaction zone and the reflected shock have the subscript 1, and those in the region between the reflected shock front and the overdriven detonation have the subscript 2, and those in the region between the overdriven detonation and the streamline have the subscript 3.

In the regular reflection process, the flow entry I with normal and tangential components deflects with a deflection angle θ_1 from its original direction, and then proceeds in a straight path to the reflected shock. In passing through this discontinuity it is again deflected upward with an angle $\theta_2 = \theta_1$ and then the flow again becomes parallel to the collision line. In region (1), we assume that region (1) meets the CJ condition.

$$P_1 = P_{CJ} = \rho_0 D_I^2/(\gamma+1) \tag{1}$$

$$\rho_1 = \rho_{CJ} = (\gamma+1)\rho_0/\gamma \tag{2}$$

$$u_1 = D_{CJ}\sqrt{[\gamma/(\gamma+1)]^2 + 1/\tan^2\psi_I} \tag{3}$$

$$M_1 = \sqrt{1 + (\gamma+1)^2/(\gamma\tan\psi_I)^2} \tag{4}$$

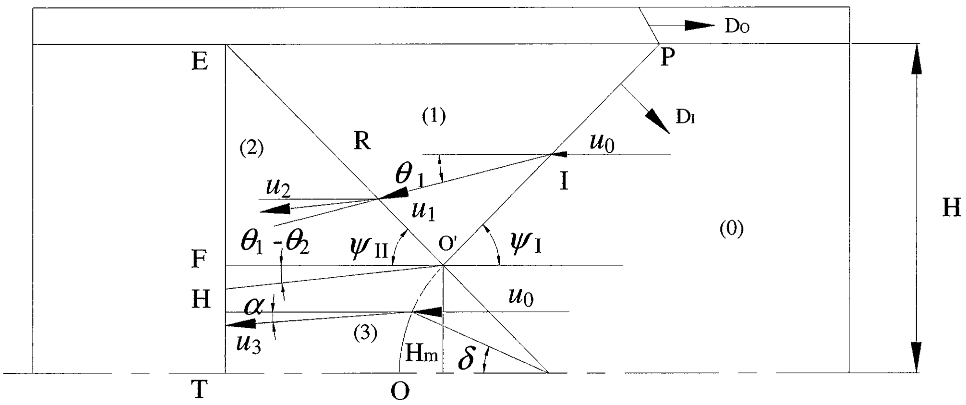

Figure 2. Flow setup used to describe Mach reflection.

where ρ_0 is the initial density, γ is the exponent of polytropic state for inner layer charge. D_{CJ}, ρ_{CJ}, and P_{CJ} are CJ detonation velocity, density, and pressure of inner charge, respectively.

As mentioned before, the detonation begins with a large incident angle ψ_I which is nearly equal to $\pi/2$. With the detonation progressing, the detonation wave will propagate with a constant value of the incident angle. The incident angle of detonation wave can be defined as

$$\sin\psi_I = D_I/D_O \tag{5}$$

The deflection angle from region (0) to region (1) is defined by

$$\tan\theta_1 = \frac{\tan\psi_I}{1+\gamma(1+\tan^2\psi_I)} \tag{6}$$

In region (2), using mass, momentum, and energy conservation, there are:

$$\frac{P_2}{P_1} = \frac{2\gamma}{\gamma+1}M_1^2\sin^2(\psi_{II}+\theta_1) - \frac{\gamma-1}{\gamma+1} \tag{7}$$

$$\frac{\rho_2}{\rho_1} = \frac{(\gamma+1)M_1^2\sin^2(\psi_{II}+\theta_1)}{(\gamma-1)M_1^2\sin^2(\psi_{II}+\theta_1)+2} \tag{8}$$

$$u_2 = \frac{\rho_1}{\rho_2}\frac{u_1\sin(\psi_{II}+\theta_1)}{\sin\psi_{II}} \tag{9}$$

The deflection angle θ_1 and $\psi_{II}+\theta_1$ satisfy the following relationship.

$$\tan\theta_1 = \frac{[M_1^2\sin^2(\psi_{II}+\theta_1)-1]\tan^{-1}(\psi_{II}+\theta_1)}{M_1^2[(\gamma+1)/2-\sin^2(\psi_{II}+\theta_1)]+1} \tag{10}$$

As the incident angle ψ_I increases and the regular reflection is limited to a certain value of ψ_I, Mach reflection would be expected to occur. As the deflection angle θ_2 is smaller than θ_1, mass will be accumulated in region (2) which forces the collision point O moving to O′. Part of the mass flows through the incident detonation front, and then through the reflected shock front, while the other part flows through the detonation front which forms the Mach stem. This reflection configuration involves four discontinuities: the incident detonation wave, the reflected shock wave, an overdriven detonation wave and a contact discontinuity between the region (3) and the region (2).

For region (2), the reflection flow is deflected from region (1) which is not parallel to the line of collision. Again referring to Figure 2, the pressure, density and flow velocity in region (2) can be written as

$$P_2 = P_1 + u_{1r}^2(v_1 - v_2)/v_1^2 \tag{11}$$

$$u_{1r} = u_1\sin(\psi_{II}+\theta_1) \tag{12}$$

$$v_2 = v_1\tan(\psi_{II}+\theta_1-\theta_2)/\tan(\psi_{II}+\theta_1) \tag{13}$$

$$u_2 = u_1\sin(\psi_{II}+\theta_1)(v_2/v_1)/\sin(\psi_{II}+\theta_1-\theta_2) \tag{14}$$

From the experimental observation of Hull [16], the Mach stem is a curved surface, normal to the symmetry axis at point O, and tangent with detonation-front (I) at point O'. The deflection angle α in Mach stem varies from point O with a value of $\alpha = 0°$ to point O' with a value of $\alpha = \theta_1 - \theta_2$, whilst the angle of the tangent line at Mach stem to symmetry axis β varies from $\pi/2$ to ψ_I. Using conservation relation of Mach stem, the parameters in region (3) can be defined as

$$P_3 = P_0 + (D_{CJ}\sin\beta/\sin\psi_I)^2(v_3 - v_0)/v_0^2 \tag{15}$$

$$\alpha = \beta - \arctan[(v_3/v_0)\tan\beta] \tag{16}$$

$$u_3 = \frac{v_3}{v_0}\frac{D_{CJ}\sin\beta}{\sin\psi_I\sin(\beta-\alpha)} \tag{17}$$

From Sternberg's definition [15], when Mach reflection occurs there is a slip line in the detonation products emanating from the triple point. This line is a streamline across a place where the pressure is continuous but the velocity and density are not. Therefore, there exists a triple point at $P_3 = P_2$. As mentioned before, mass accumulation in region (2) is the main reason of Mach stem. The flow at triple point in region (3) is both from mass flow of region (2) in vertical direction and region (0) in horizontal direction. The parameters in region (3) at triple point is given by

$$u_{3t} = [u_0 \cos\psi_\mathrm{I} + u_2 \sin(\theta_1 - \theta_2)\cos\psi_\mathrm{I}]/\cos[\psi_\mathrm{I} - (\theta_1 - \theta_2)] \tag{18}$$

$$\rho_{3t} = \frac{[u_0\rho_0 \sin\psi_\mathrm{I} + u_2\rho_2 \sin(\theta_1 - \theta_2)\cos\psi_\mathrm{I}]}{[\sin[\psi_1 - (\theta_1 - \theta_2)]/u_{3t}}. \tag{19}$$

$$P_{3t} = D_\mathrm{CJ}^2 (v_0 - v_{3t})/v_0^2 \tag{20}$$

From Eqs. (11–14) and Eqs. (18–20), values of P_2, u_2, $\rho_2(v_2)$, θ_2, ψ_II, u_{3t}, and ρ_{3t} can be determined.

For the parameters at collision point O ($\beta = 90°$), there are three indeterminate values (P_3, v_3, and u_3) but only two formulas of Eqs. (15) and (17). An additional equation should be used to determine above values at collision point. Consulting Mader's results [17], the state equation of the detonation products is assumed in the form of $P = P(E,v)$, where P is the pressure, E the specific internal energy, and v is the specific volume ($1/\rho$). The detonation state variables behind the detonation front are found by solving the system

$$P = P(E, v) = \left(Av^{-1} + Bv^{-2}\right)E + Cv^{-3} \tag{21}$$

$$E = E_0 + (p + p_0)(v_0 - v)/2 \tag{22}$$

where the subscript zero refers to the undetonated explosive.

2.3 Computational Results for Detonation Reflection in DLC Charge

In order to have a detailed understanding of detonation wave propagation in DLC charges, the reflection parameters are determined using the above equations. Here, we take TNT ($\rho_0 = 1.63\ \mathrm{g\,cm^{-3}}$) as inner charge for example, the CJ detonation parameters are $\gamma = 2.856$, $D_\mathrm{CJ} = 6973\ \mathrm{m\,s^{-1}}$, $E_\mathrm{CJ} = 7 \cdot 10^6\ \mathrm{Pa\ m^3\,kg^{-1}}$. Using related experimental data for TNT, the values obtained for A, B, C in Eq. (21) are $A = 0.3501$, $B = 7.02 \cdot 10^{-5}\ \mathrm{m^3\,kg^{-1}}$, $C = 1.18\ \mathrm{Pa\ m^9\,kg^{-3}}$. Using the methods of Dunne [13], the critical Mach reflection angle is determined to be 45.6° for TNT.

As shown in Figure 3, pressures at triple point O′ and collision point O with different incident angle ψ_I are first determined. From Figure 3, we can see that the ratio of the pressure behind the reflected shock to P_CJ during regular reflection is about 2.4. As the incident angle ψ_I increases (larger ratio of $D_\mathrm{I}/D_\mathrm{O}$), Mach reflection occurs and the pressure at collision point increases suddenly to about 3.5 times of P_CJ with critical Mach reflection angle

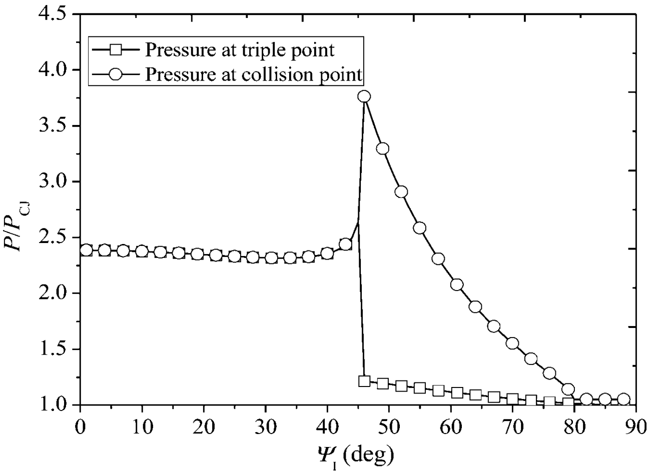

Figure 3. The calculated pressure versus incident angle at triple and collision point.

ψ_I and then decreases with increasing of ψ_I. As the incident angle increases to about 80°, pressure at triple and collision point are both equal to P_CJ. This means the DLC charge becomes expansion detonation with large value of incident angle.

The reflection and deflection angle for detonation propagation in inner charge are shown in Figure 4. The reflection angle ψ_II increases as incident angle increases in regular reflection. Due to mass accumulation at region (2), with the collision point moving to the triple point O', the reflection angle is discontinuous at the critical Mach reflection angle ψ_I. The deflection angle θ_1 increases at low incident angle and reach the maximum value at 52° of the incident angle, then decreases to zero at 90°. The deflection angle θ_2 has maximum value at the critical Mach reflection angle ψ_I, which means θ_1–θ_2 begin with its maximum value at the critical Mach reflection angle and decreases to zero at $\psi_\mathrm{I} = 90°$.

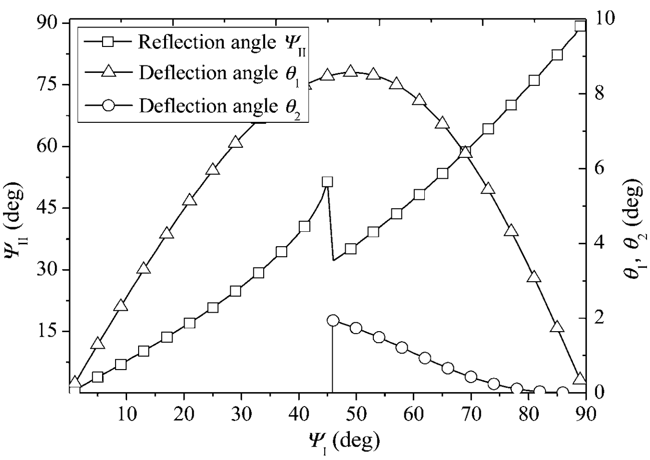

Figure 4. The calculated reflection angle and deflection angle versus incident angle.

From the discussion above, Mach reflection is the main reason of overdriven detonation in the inner layer charge, and the parameters in Mach stem are determined based on Eqs. (15–17) and Eqs. (21–22). Calculated pressure in Mach stem versus tangent of angle β of curved Mach stem for different incident angles is shown in Figure 5. Pressure increases with central angle of curved Mach stem and the maximum value, 4.0 times of P_{CJ}, is reached at an incident angle of 46°. As shown in Figure 6, the flow velocity decreases, while the density increases with increasing central angle.

2.4 Mach Stem Height Prediction

There are many experimental results and numerical prediction of reflection of detonation wave in the related literature [12,13,18,19]. To date there is no accurate method of predicting the height of Mach stem in irregular reflection of detonation wave. An accurate prediction of the Mach stem height is not only useful in understanding

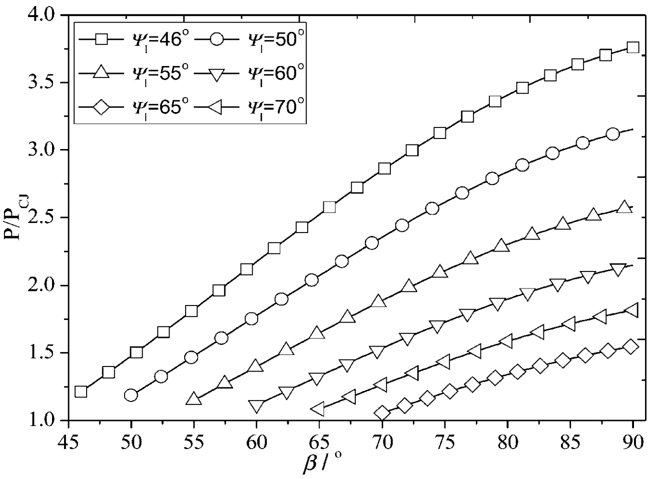

Figure 5. The calculated pressure in Mach stem.

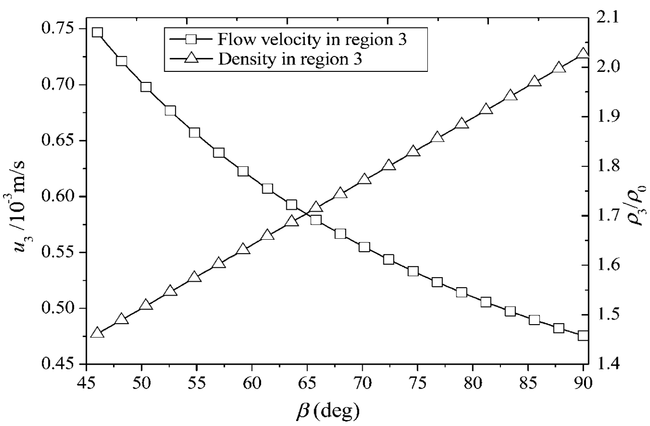

Figure 6. Flow velocity and density in Mach stem at incident angle of 46°.

the behavior of the shock reflection in condensed HE but also important in the design of DLC charge.

The problem setup is shown graphically in Figure 2. As mentioned before, the Mach reflection in condensed HE is induced by compression of region (2). Due to Mach reflection of detonation wave in inner charge, the income mass flow is divided into two parts. The first part flows though PO' and flows out EH for reflection in region (2), and the second part flows though O'O and flows out TH for Mach reflection in region (3). The mass flow is equated to the mass flow through EH and TH corresponding to $u_2\rho_2$ and $u_3\rho_3$, respectively. We assume H_m is the Mach stem height and ET = H is the diameter of the inner charge. Equating the two mass fluxes produces the following equations

$$\rho_0 u_0 \pi (H - H_m)^2 \frac{\sin\psi_I}{\sin(\psi_I - \theta_1)} + \rho_0 u_0 \pi H_m^2 = \rho_2 u_2 \cos(\theta - \varepsilon)\pi \mathrm{EH}^2 \frac{\sin(\psi_{II} + \theta_1 - \theta_1)}{\sin(\psi_{II} + \theta_1)} + \int \rho_3(\alpha) u_3(\alpha) \cos\alpha \mathrm{d}s \quad (23)$$

EH can be written as

$$\mathrm{EH} = (H - H_m) + \frac{(H - H_m)}{\tan(\psi_{II})}\tan(\theta_1 - \theta_2) \quad (24)$$

The flow which passes through the Mach stem has a higher temperature, a greater increase in density and entropy, and a lower particle velocity than the flow which passes through the detonation front and reflected shock. So the mass flow though Mach stem is the integration at the curved Mach stem.

$$\int \rho_3 u_3 \cos\alpha \mathrm{d}s = \int_0^{\pi/2-\psi_I} \rho_3(\delta) u_3(\delta) \cos\alpha \cdot s(\delta) \mathrm{d}\delta \quad (25)$$

where δ is the central angle of the curved Mach stem, α is the deflection angle behind Mach stem.

Using numerical solution of integral equations $s(\delta)$ can be written as:

$$\begin{aligned} s(\delta) = \pi\Big[&H_m \sin\delta/\cos\psi_I - \big(H_m \tan\psi_I + (H - H_m)/\tan\psi_{II} \\ &- H_m \cos\delta/\cos\psi_I\big)\tan\alpha(\delta)\Big]^2 \\ &- \pi\Big[H_m \sin(\delta + d\delta)/\cos\psi_I - \big(H_m \tan\psi_I \\ &+ (H - H_m)/\tan\psi_{II} - H_m \cos(\delta + d\delta)/ \\ &\cos\psi_I\big)\tan\alpha(\delta + d\delta)\Big]^2 \end{aligned} \quad (26)$$

Take $\Delta H = H_m/H$ as the indeterminate in Eqs. (23–25) and Eq. (26).

The Eqs. (23–26) are solved based on the calculated results in Section 2.3. Among the calculated parameters, the most interesting one is the Mach stem height corresponding to different initial conditions. Comparable results of

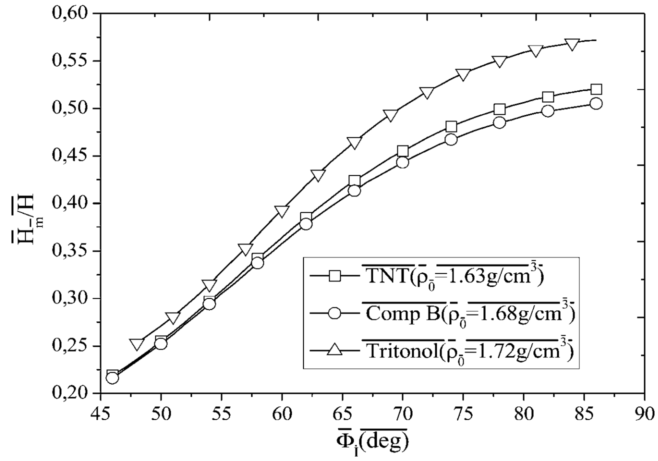

Figure 7. Calculated Mach stem height versus incident angle with different inner HE.

Table 1. Parameters of some HEs with lower detonation velocity.

High Explosive	ρ_0 (g cm^{-3})	D_{CJ} (m s^{-1})	P_{CJ} (GPa)	γ
TNT	1.63	6930	20.30	2.856
Comp B(RDX/TNT(60/40))	1.68	7840	29.45	2.630
Tritonol (TNT/Al(80/20))	1.72	6700	25.65	2.010

the normalized Mach stem height H_m/H with different initial conditions are shown in Figure 7. Parameters of three different HEs with lower detonation velocity are shown in Table 1. The results show that Mach stem height increases with incident angle. The Mach stem height based on the present prediction is about $0.22H$ near critical Mach reflection angle. This indicates that regular reflection to Mach reflection transition takes place with discontinuous variation. The predicted values of the Mach stem heights are slightly higher for lower values of the polytropic exponent for inner charge.

3 Numerical Simulation of Detonation Wave Propagation in DLC Charges

3.1 Numerical Simulation Model

Detonation phenomena occur on the microsecond time scale, and simulation of detonation process usually requires large deformation of grid. In this case, the appropriate equations that describe the material response are the Euler equations, which describe the conservation of mass, momentum, and energy for an inviscid, compressible fluid. Euler codes model perforation as a hydrodynamics event, providing a robust characterization of multi-material movement, at the cost of complex mixed-cell thermodynamics and interface tracking algorithms. An inordinately fine mesh may be required to model detonation products transport. In the present paper, Euler codes were used to describe the detonation and shock induced initiation of HE. Figure 8 shows the finite element model of the simulation. Since the model is an axial symmetry question, we only need to build up a two-dimension axial symmetry model. The inert material shaper was used to get an initial annular detonation wave.

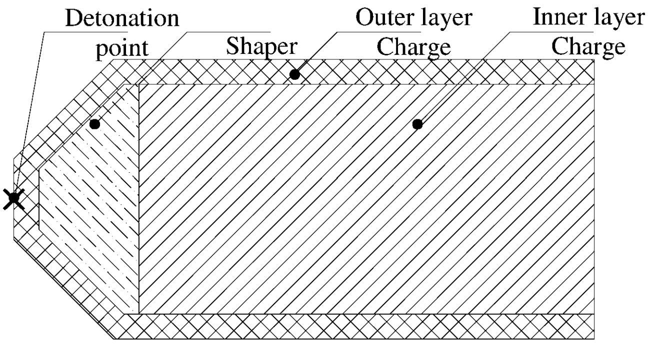

Figure 8. Numerical simulation model of double-layer charge.

3.2 Ignition and Growth Model

Traditionally, the reaction models which are used for condensed HE are divided into two common categories [20]. The first is the prescription model where the arrival time of the detonation wave is assigned a priori. The compression and reaction front comprising the detonation wave are treated as a single front. Program Burn and Detonation Shock Dynamics models are two typical examples of this category. They pre-define the pressure as a function of relative volume and internal energy per initial volume, and the lighting time is computed at beginning of initiation. These models are very useful in solving engineering problems because the grid resolution requirements are not as stringent as other options. However, one trait of these models is that they typically do not resolve the von Neumann pressure spike and reaction zone associated with the detonation front. Such resolutions can be key issues in certain problems such as the interaction of detonation waves with metal.

The second category model is kinetic based reaction schemes. These models include the reaction process in an explicit manner. The progression of the reaction is dictated using a rate law that is dependent on variables such as pressure and temperature. This class of models is similar to the kinetics schemes commonly used in gas phase combustion simulations. A popular kinetics scheme that has been successfully used for the detonation problem is the Ignition and Growth Model proposed by Lee and Tarver [21,22].

The Ignition and Growth Model is a Zeldovich-von Neumann-Döring (ZND) model as described by Fickett and Davis 2000 [23]. This class of model treats the shock of the detonation front as a discontinuous and explicit reaction process behind the shock. The level of resolution of the reaction front will depend on numerical aspects of the hydrocode used.

Table 2. JWL EOS parameters for TNT and detonation products.

Parameters	Unreated explosive	Detonation products
ρ_0 ($g\,m^{-3}$)	1.63	–
A (GPa)	1798	371.2
B (GPa)	−93.1	3.23
R_1	6.2	4.15
R_2	3.1	0.95
ω	0.8921	0.3
C_V ($GPa\,K^{-1}$)	1.540E-3	1.0E-3
T_0 (K)	298	–
E_0 (GPa)	0	7.0

Table 3. Rate parameters for TNT.

Parameters	Value	Parameters	Value
I	50	a	0.02
G_1	0.00	E_0	0.081
y	2.0	G_2	40.0
d	0.667	g	0.222
C	0.222	e	0.00
C_p	1.0E-5	z	1.20
C_v	2.487E-5	F_{max}	1.00
x	4.0	F_{min}	1.00

A JWL equation of state defines the pressure in the unreacted explosives as [24]

$$P_e = r_1 e^{-r_4 V_e} + r_2 e^{-r_5 V_e} + r_3 \frac{T_e}{V_e}\left(r_3 = \omega_e C_{vp}\right) \tag{27}$$

Another JWL equation of state defines the pressure in the reaction products as

$$P_p = a e^{-r_{p1} V_p} + b e^{-r_{p2} V_p} + r_{p3} \frac{T_p}{V_p}\left(g = \omega_p C_{vp}\right) \tag{28}$$

where V_e, V_p, T_e, T_p are relative volume and temperature of unreacted explosive and reactive products, respectively.

The chemical reaction rate for conversion of unreacted explosive to reaction products consists of three physically realistic terms: an ignition term in which a small amount of explosive reacts soon after the shock wave compression, a slow growth of reaction as this initial reaction spreads, and a rapid completion of reaction at high pressure and temperature. The form of the reaction rate equation is

$$\begin{aligned}\frac{\partial F}{\partial t} &= I(1-F)^b(\rho/\rho_0 - 1 - a)^x \\ &\quad + G_1(1-F)^c F^d p^y + G_2(1-F)^e F^g p^z\end{aligned} \tag{29}$$

3.3 Material Model Parameters

Several HEs with different detonation velocity are used in numerical simulation. Casted TNT with lower detonation velocity is used as inner charge, and the ignition and growth model is used to describe the shock induced initiation and detonation wave interaction. Table 2 shows the JWL EOS parameters for TNT and detonation products, and Table 3 gives the shock induced initiation rate parameters.

Table 4. JWL EOS parameters for outer layer explosive.

Parameters	HMX	PBX 9404	RDX-inert	Comp B
ρ_0 ($g\,cm^{-3}$)	1.891	1.84	1.700	1.717
D_{CJ} ($m\,s^{-1}$)	9110	8800	8425	7980
P_{CJ} (GPa)	42	37	29.6	29.5
D_O/D_I	1.31	1.27	1.22	1.15

Four explosives with different detonation velocities (from 7980–9110 $m\,s^{-1}$) are used as outer layer charge. JWL EOS parameters are shown in Table 4.

3.4 Typical Detonation Wave in DLC Charge

The inner layer charge is shielded by a cone of nylon to prevent direct coupling of the detonation wave into the charge and initiated by annular detonation wave. The outer layer charge has a thickness of 5 mm, which is larger than critical detonation diameter. Typical detonation propagation was simulated using different ratios of detonation velocity at time of 9, 15, and 25 μs. Figure 9(a) shows the detonation wave propagation in an ordinary cylindrical charge. Figures 9(b) and (c) show the detonation wave propagation with Mach reflection and regular reflection, respectively.

The detonation wave in an ordinary charge propagates with a convergent shape at beginning of initiation. As detonation is progressing, it propagates with a spherical shape of nearly constant curvature. The detonation front of the outer layer charge in DLC is clearly prior to the inner charge. From this detonation front a conical detonation wave runs into the inner charge. There are two cases of detonation wave in the inner charge. As the incident angle has a higher value than the critical angle for Mach reflection, there is obviously a Mach stem with higher pressure near the axis of inner layer charge which is shown in Figure 9(b). As the incident angle is smaller than the critical angle of Mach reflection, there is a conical convergent detonation wave in the inner charge. With the detonation progressing, detonation wave with the regular reflection and Mach reflection in the inner charge both propagates in steady state which includes the shape, velocity, and pressure. Figure 10 shows a typical pressure history at collision point of detonation wave to symmetry line for DLC charge and ordinary charge. From these results we can see that overdriven detonation occurs in inner layer charge, and maximum transmitted pressure, 70 GPa, is shown to occur at collision point during Mach reflection.

Comparisons between the simulations and the present predictions for several DLC charges are shown in Table 5. Calculated incident angles and pressure at collision point in Mach reflection from the present model agree well with the corresponding numerical results. The

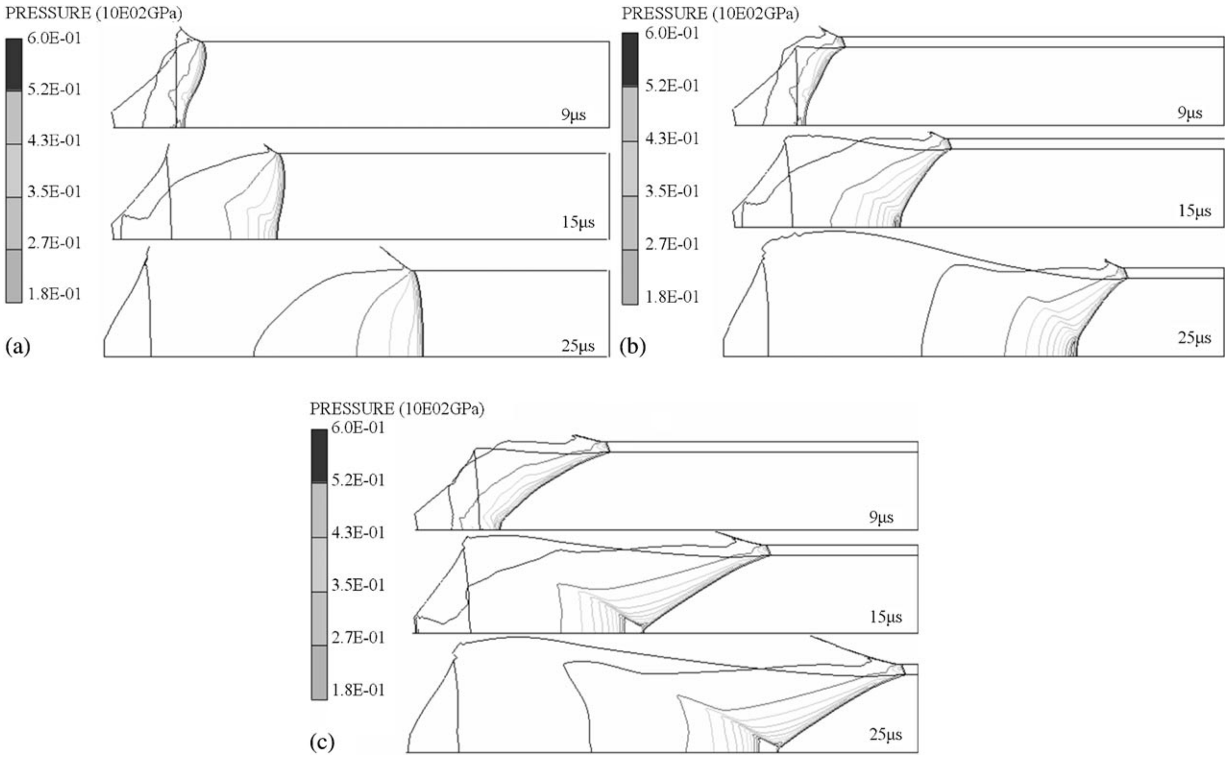

Figure 9. Detonation process of double layer charge (a) Ordinary charge, (b) Mach reflection in DLC charge, (c) regular reflection in DLC charge.

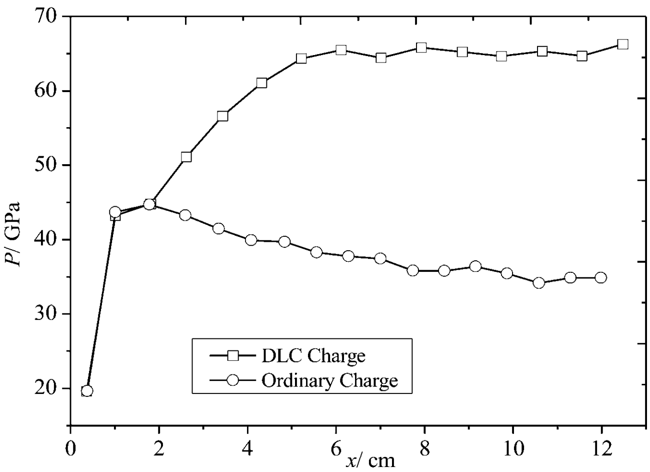

Figure 10. Pressure at collision point of symmetry line.

predicted values of the normalized Mach stem heights H_m/H are slightly lower than the numerical simulations especially for larger values of the incident angle. In spite of the fact that the assumptions used for the present predictions may introduce errors to some extent, the main reason is likely attributed to neglect expansion of detonation products.

4 Conclusion

Detonation wave propagation in DLC charge has been discussed in this paper. The regular and Mach reflection configurations as well as the resulting flow field in steady flow have been analyzed and formulated. Flow parameters are determined based on the assumption of continuous pressure at triple point. Non-parallel flow of region (2) to axial line creates Mach stem and mass conservation has been used to determine the Mach stem heights. The

Table 5. Comparison simulation and model predictions.

Type	D_O/D_I	Ψ_I (°)		H_m/H		P_m (GPa	
		Simulation	Eq. (5)	Simulation	Eqs. (23–26)	Simulation	Eqs. (15–17) Eqs. (21–22)
Comp B-TNT	1.15	59.47	60.28	0.435	0.365	47.82	43.35
RDX(inert)-TNT	1.22	56.61	55.10	0.373	0.305	53.99	52.37
PBX9404-TNT	1.27	53.97	51.95	0.305	0.273	61.47	59.27
HMX-TNT	1.31	50.09	49.53	0.285	0.252	66.91	64.24

corresponding numerical simulation based on the Lee–Tarver model has been carried out using DLC charge to have a contrast to normal charge. It has been found that for a given DLC charge the Mach stem heights are solely determined by difference of the detonation velocity. It has also be shown that the Mach stem height is 0.22 near the critical Mach reflection angle, which means regular reflection to Mach reflection transition takes place with discontinuous variation. The results show that the analysis results correlate well with the corresponding numerical results, also double layer charge is an efficient way to improve performance of HE charge.

Symbols and Abbreviations

P	Pressure (GPa)
u	Flow velocity ($m\,s^{-1}$)
ρ	Density($g\,cm^{-3}$)
γ	The exponent in polytropic of state
M	Mach number of detonation wave
E	Specific internal energy of HE ($J\,kg^{-1} = Pa\ m^3\,kg^{-1}$)
v	Specific volume ($m^3\,kg^{-1}$)

Acknowledgments

The research works are support by the Youth Scholarship Foundation of Nanjing University of Science & Technology and National Natural Science Foundation of China (NSFC10902053). The author would like to thank Prof Huiwu Chen(NJUST) for his support and encouragement, and Dr. Xiaoning Zhao(NJUST) for his simulation assistance.

References

[1] F. Müller, Mach-reflection of Detonation Waves in Condensed High Explosives, *Propellants, Explos., Pyrotech.* **1978**, *3*, 115.

[2] M. Held, Behavior of Dual Composition Explosive, *EURO-PYRO 1995*, 6th International Congress on Pyrotechnics, June **1995**, Tours, France, p. 185.

[3] G. A. Adadurov, A. N. Dremin, G. I. Kanel, Mach Reflection Parameters for Plexiglas Cylinders, *Zhurnal Prikladnoi Mekhanikii Tekhnicheskoi Fiziki* **1969**, *10*, 126.

[4] Z. Liu, S. Nagano, S. Itoh, Overdriven Detonation Phenomenon in High Explosive, *Shock Compression Condens. Matter* **1999**, 227.

[5] Z. Liu, K. Tanaka, S. Itoh, A Method for Producing Extra-high Dynamic Pressure due to the Efficient Use of High Explosive, *J. Pressure Vessel Technol.* **2004**, *126*, 264.

[6] Z. Liu, S. Kubota, S. Itoh, Numerical Study on Hypervelocity Acceleration of Flyer Plates by Overdriven Detonation of High Explosive, *Int. J. Impact Eng.* **2001**, *26*, 443.

[7] Z. Liu, Overdriven Detonation Phenomenon and Its Application to Ultra-high Pressure Generation, *Doctoral Dissertation*, Kumamoto University, Japan March, **2001**.

[8] M. Otsuka, H. Morimoto,, S. Nagano, S. Itoh, Effective Use of Overdriven Detonation in High Explosives, in: C. Cavailler, G. P. Haddleton, M. Hugenschmidt (Eds.), *25th International Congress on High-Speed Photography and Photonics*, Proc. SPIE 4948, **2003**, p. 464, doi: 10.1117/12.516938.

[9] S. Itoh, Visualization of an Overdriven Detonation Phenomenon in a High Explosive, *J. Flow Visual. Image Process.* **1999**, *6*, 295.

[10] T. Hamada, S. Itoh, H. Kato, An Investigation on Overdriven Detonation Phenomenon in Concentric Double Cylindrical High Explosive, *Mater. Sci. Forum* **2004**, *465–466*, 379.

[11] H. Kato, K. Murata, S. Itoh, Application of Overdriven Detonation in High Density Explosive to Shaped Charge, *23rd International Symposium on Ballistics*, Tarragona, Spain, April 16–20, **2007**, p. 223.

[12] X.-f. Zhang, J.-b. Ding, X.-n. Zhao, Numerical Simulation of Double Layer Shaped Charge, *Explosion Shock Waves* **2009**, *30*, 623 (in Chinese).

[13] B. B. Dunne, Mach Reflection of Detonation Waves in Condensed High Explosive, *Phys. Fluids* **1961**, *4*, 918.

[14] B. B. Dunne, Mach Reflection of Detonation Waves in Condensed High Explosive II, *Phys. Fluids* **1964**, *7*, 1707.

[15] H. M. Sternberg, D. Piacesi, Interaction of Oblique Detonation Waves with Iron, *Phys. Fluids* **1966**, *9*, 1307.

[16] L. M. Hull, Mach Reflection of Spherical Detonation Waves, *10th International Detonation Symposium*, Boston, Massachusetts, July 12–16, **1993**.

[17] C. L. Mader, One and Two-dimensional Flow Calculations of the Reaction Zones of Ideal Gas, Nitromethane, and Liquid TNT Detonations, *12th Symp. (Int.) Combust.* Poitiers, France, July 14–20, **1969**, *12*, 701.

[18] S. K. Andilevko, On Detonation of an Explosive Layer, *J. Eng. Phys. Thermophys.* **2001**, *74*, 150.

[19] S. Krishnan, C. Brochet, R. Cheret, Mach Reflection in Condensed Explosives, *Propellants, Explos., Pyrotech.* **1981**, *6*, 170.

[20] J. K. Clutter, D. Belk, Simulation of Detonation Wave Interaction Using an Ignition and Growth Model, *Shock Waves* **2002**, *12*, 251.

[21] G. Oliveira, *Numerical Studies of the Behavior of Heterogeneous Explosives Using the Ignition and Growth Model,* Doctoral Dissertation, Rensselaer Polytechnic Institute Troy, New York, **2006**.

[22] E. L. Lee, C. M. Tarver, Phenomenological Model of Shock Initiation in Heterogeneous Explosives, *Phys. Fluids* **1980**, *2*, 2362.

[23] W. Fickett, W. C. Davis, *Detonation: Theory and Experiment*, Dover Publications Inc. Mineola, NY, **2011**, Originally published: University of California Press, Berkeley **1979**.

[24] M. J. Murphy, E. L. Lee, Modeling Shock Initiation in Composition B, *10th International Detonation Symposium*, Boston, Massachusetts, July 12–16, **1993**, p. 965.

